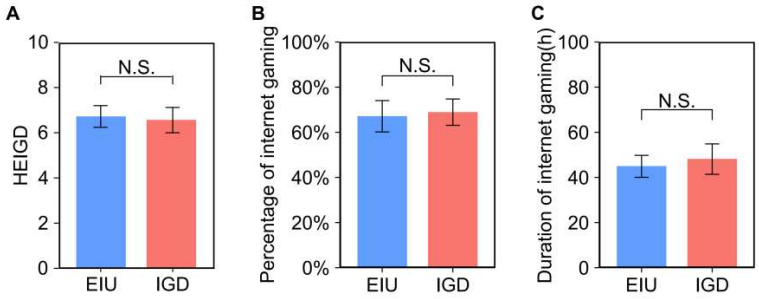


**Figure S1. Comparisons between EIU and IGD on the use of internet games.** (A) Comparison between EIU and IGD on HEIGD score. (B) Comparison between EIU and IGD on the percentage of internet gaming time in leisure time. (C) Comparison between EIU and IGD on the duration of internet gaming in a week. These indices are based on participants' recall of the status when their excessive online gaming behavior was most intense in the past year. Data are represented as mean +/- standard error. N.S. represent no significance.

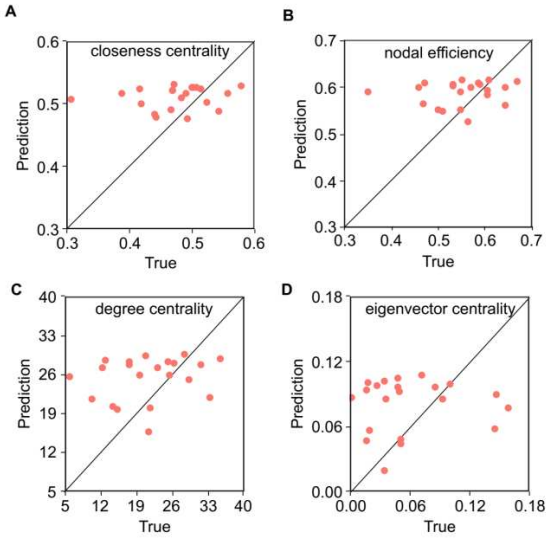


**Figure S2. Predictions and true values of hubness measures at the right ORBsupmed node in IGD.** (A) Predictions of closeness centrality were plotted against true values. (B) Predictions of nodal efficiency were plotted against true values. (C) Predictions of degree centrality were plotted against true values. (D) Predictions of eigenvector centrality were plotted against true values.

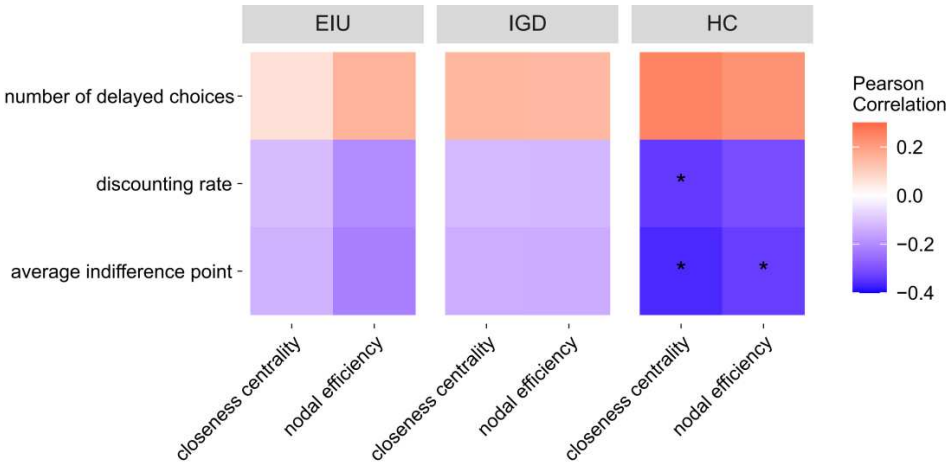


**Figure S3. Relationship between closeness centrality or nodal efficiency of the right ORBsupmed and impulsivity in decision-making in each single group.** The number of delayed choices were positively correlated with closeness centrality and nodal efficiency of the right ORBsupmed in each group. The discounting rate and average indifference point were negatively correlated with closeness centrality and nodal efficiency of the right ORBsupmed in each group. Colors represent Pearson correlation coefficients, and * represents $p < 0.05$. One-side test was used.

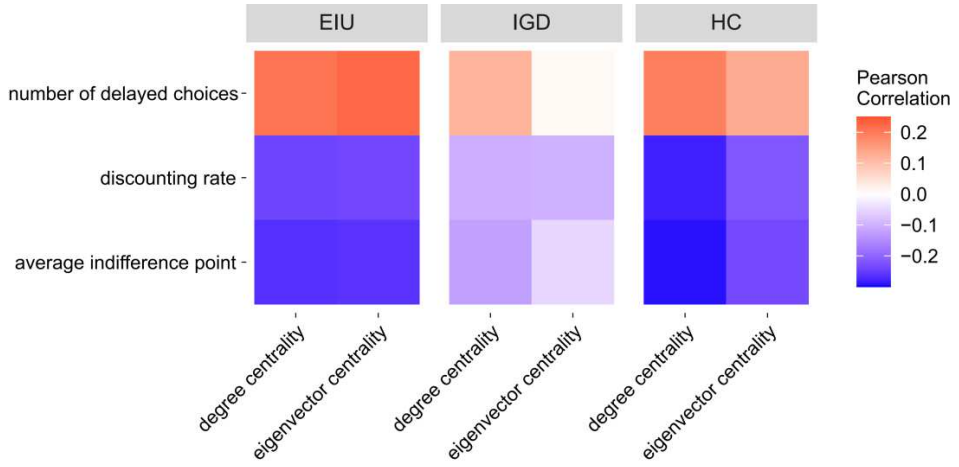


**Figure S4. Relationship between degree centrality or eigenvector centrality of the right ORBsupmed and impulsivity in decision-making in each single group.** Number of delayed choices was positively correlated with degree centrality and eigenvector centrality of the right ORBsupmed in each group. Discounting rate and average indifference point were negatively correlated with degree centrality and eigenvector centrality of the right ORBsupmed in each group. Colors represent Pearson correlation coefficients.

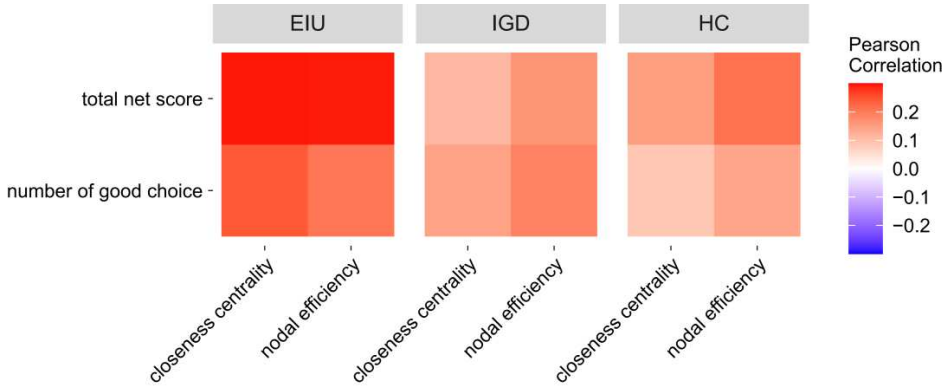


**Figure S5. Relationship between performance in IGT and closeness centrality or nodal efficiency of the right ORBsupmed in each single group.** Both number of good choices and total net score were positively correlated with closeness centrality and nodal efficiency of the right ORBsupmed in each group. Colors represent Pearson correlation coefficients.

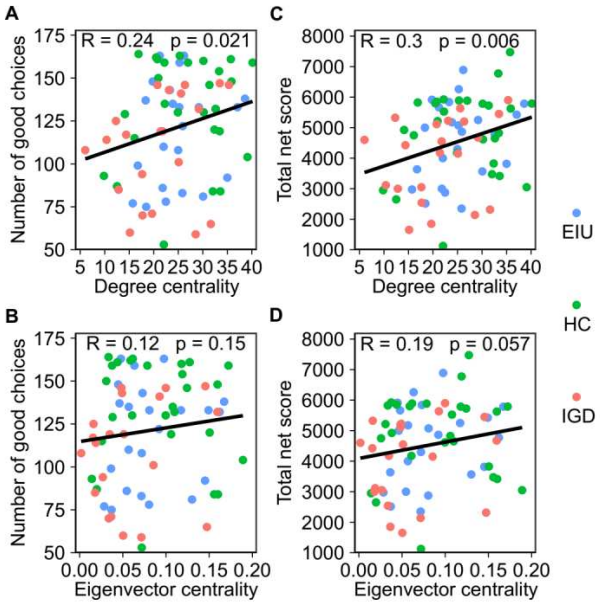


**Figure S6. Relationship between performance in IGT and degree centrality or eigenvector centrality of the right ORBsupmed.** (A) The number of good choices was plotted against the degree centrality of the right ORBsupmed. (B) The number of good choices was plotted against the eigenvector centrality of the right ORBsupmed. (C) Total net score was plotted against the degree centrality of the right ORBsupmed. (D) Total net score was plotted against the eigenvector centrality of the right ORBsupmed.

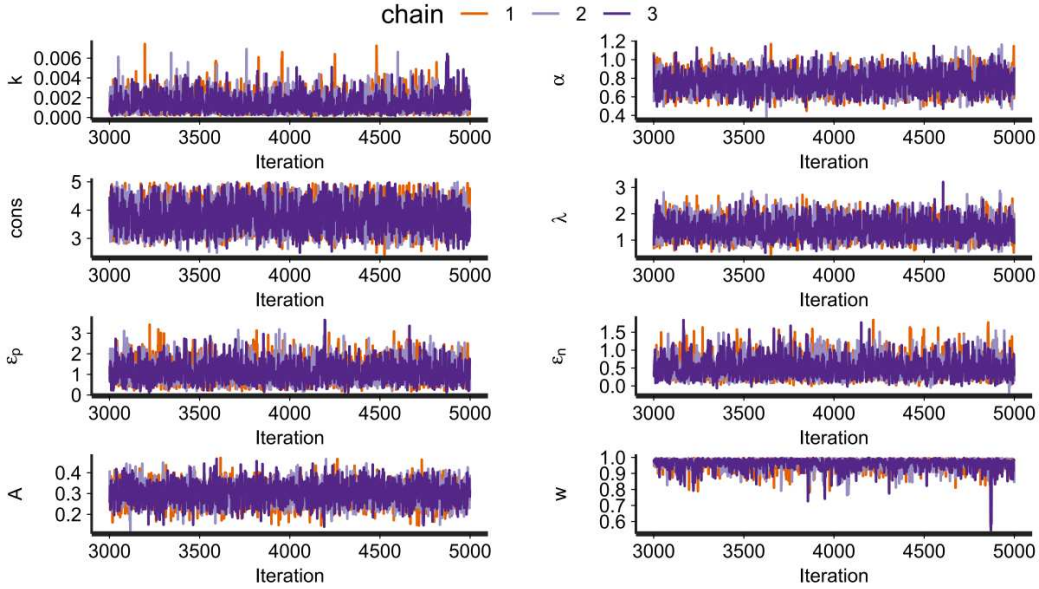


**Figure S7. Trace plot of the MCMC samples of HC group-level parameters in VPP model.** The first 3000 iterations were not plotted since they were burn-in samples. MCMC samples were well mixed and converged, which was consistent with their $\hat{R}$ values.

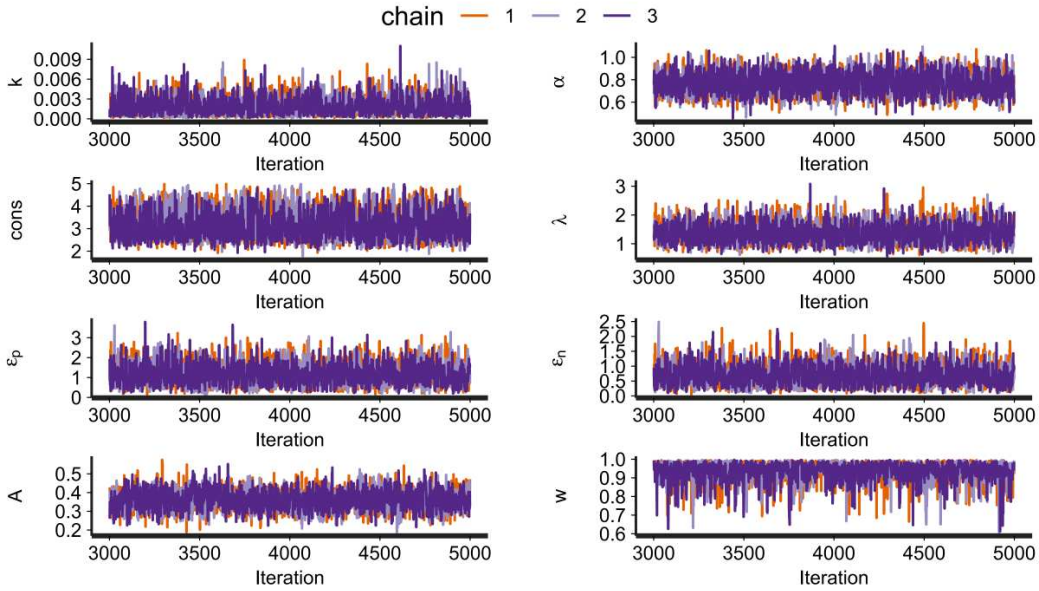


**Figure S8. Trace plot of the MCMC samples of IGD group-level parameters in VPP model.** The first 3000 iterations were not plotted since they were burn-in samples. MCMC samples were well mixed and converged, which was consistent with their $\hat{R}$ values.

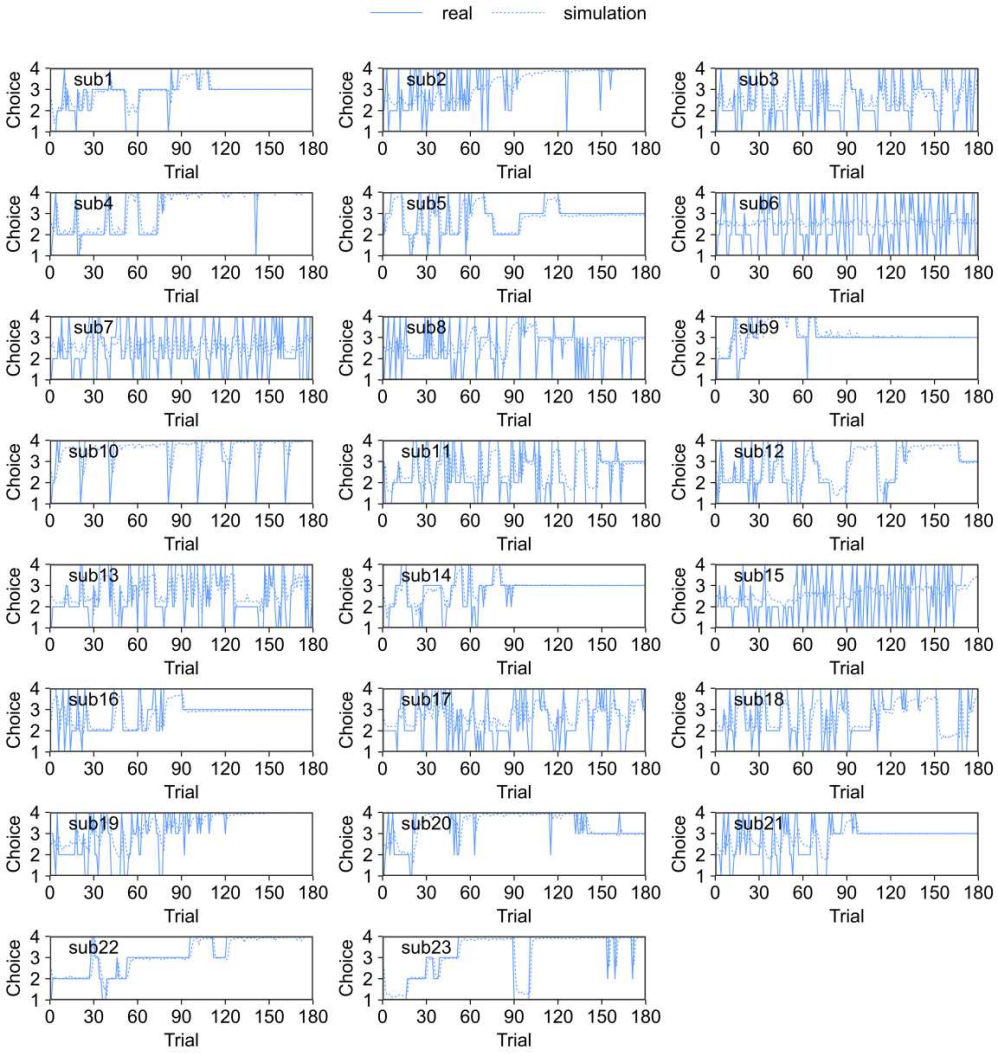


**Figure S9. Simulations of the VPP model in each single subject in EIU group.** Solid line represents real choice in each trial. Dashed line represents simulated choice in each trial.

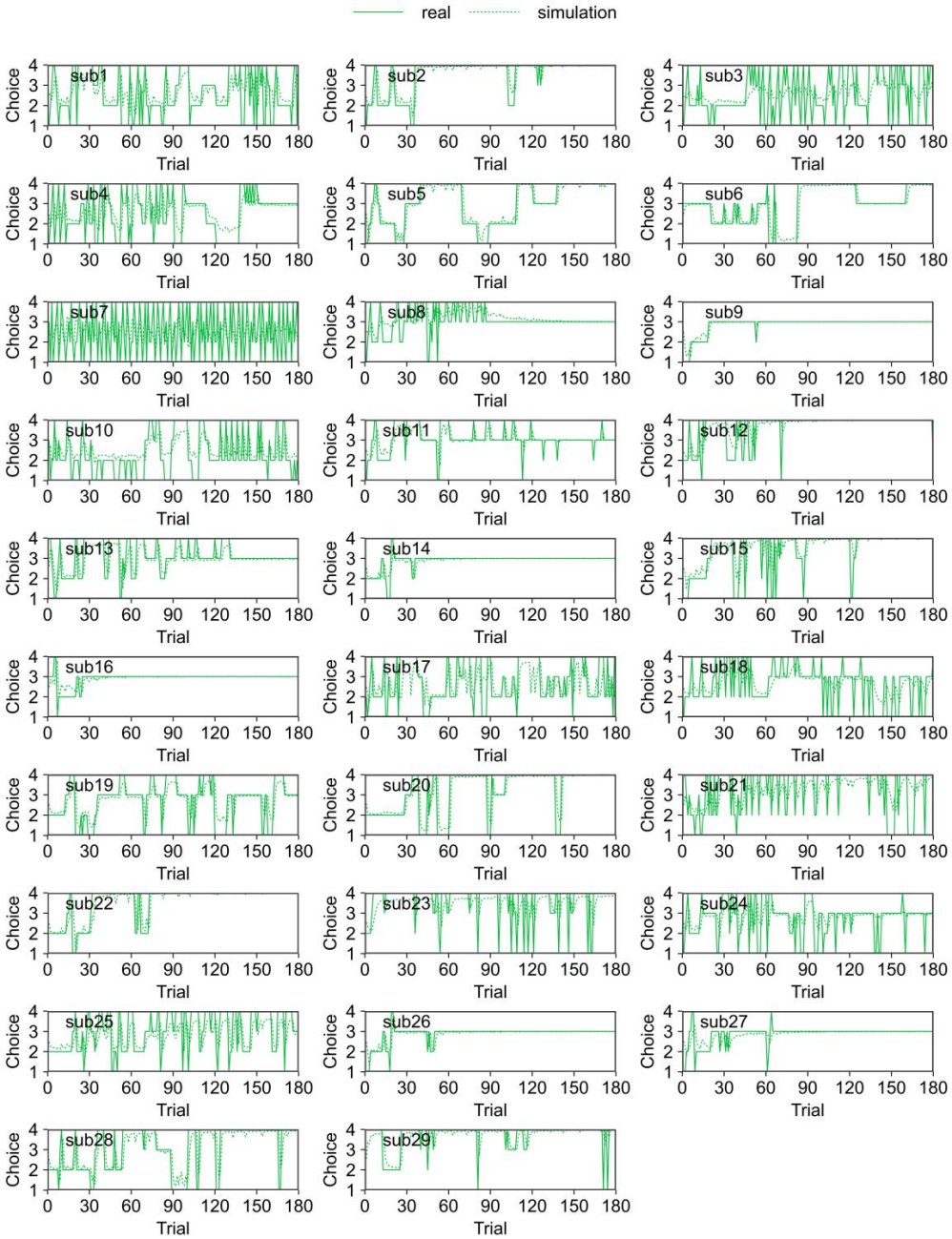


**Figure S10. Simulations of the VPP model in each single subject in HC group.** Solid line represents real choice in each trial. Dashed line represents simulated choice in each trial.

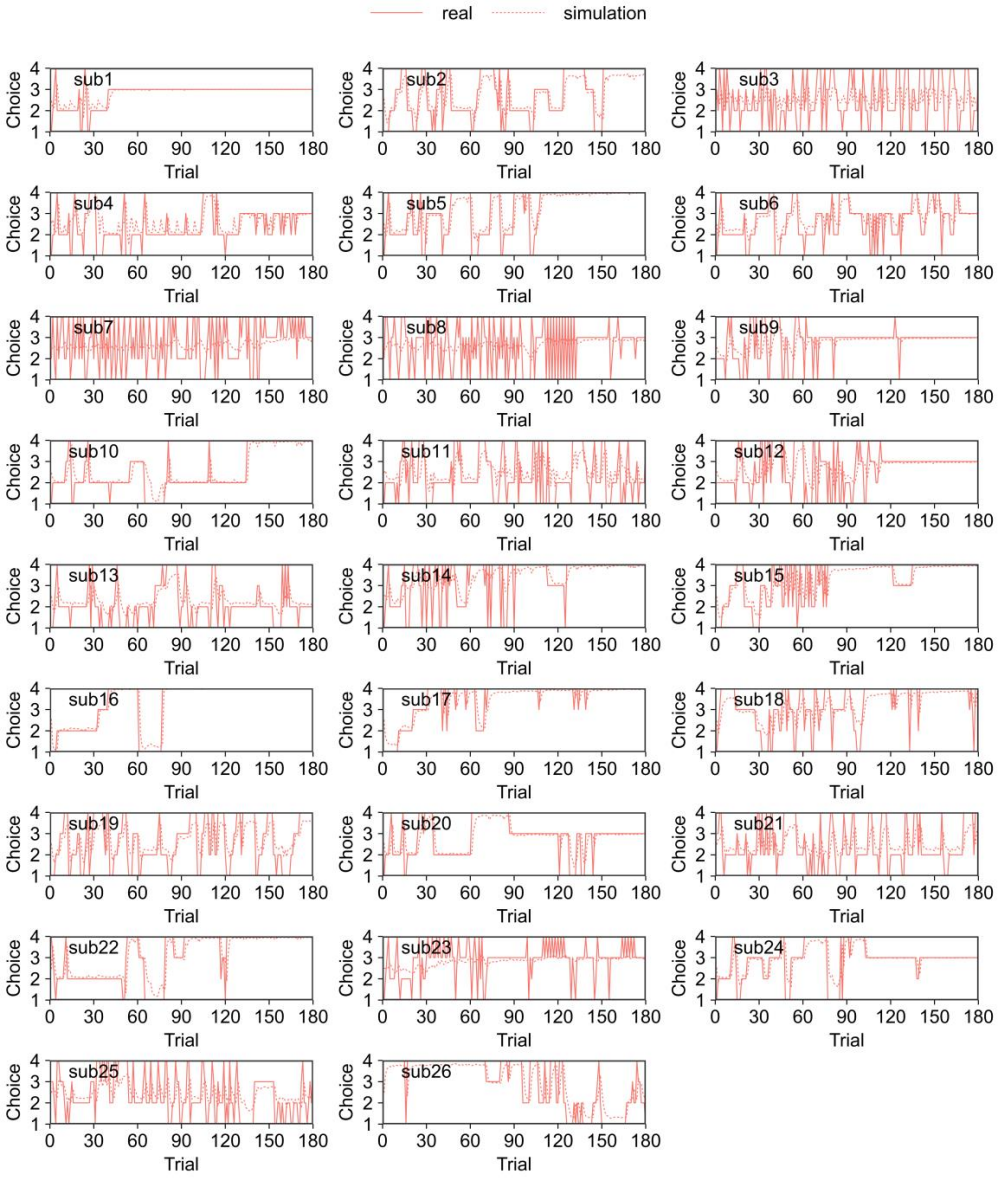


**Figure S11. Simulations of the VPP model in each single subject in IGD group.** Solid line represents real choice in each trial. Dashed line represents simulated choice in each trial.

**Table S1. Gelman-Rubin statistics of the sampling chains**

| Model | $\hat{R}$ (EIU) | $\hat{R}$ (HC) | $\hat{R}$ (IGD) |
|---|---|---|---|
| PVL-Decay | 1.000~1.003 | 1.000~1.089 | 1.000~1.003 |
| PVL-Delta | 1.000~1.006 | 1.000~1.053 | 1.000~1.100 |
| VPP | 1.000~1.013 | 1.000~1.002 | 1.000~1.026 |
| ORL | 1.000~1.004 | 1.000~1.002 | 1.000~1.005 |

## Scoring rules of HEIGD and CEIGD

Each item in the EIGD questionnaire is scored on a scale of 0 to 5, with 0 being "never" and 5 being "always". Higher score indicates higher degree of internet gaming. For the evaluation of CEIGD, participants were asked to fill the EIGD questionnaire based on their status in the last week. The sum of the score of each item was used as CEIGD. For the evaluation of HEIGD, participants were asked to fill the EIGD questionnaire based on their recall of the status when their excessive online gaming behavior was most intense in the past year. Considering that the period participants recalled was long ago and the scores they gave may not be very accurate, we first applied thresholding to the score of each item (score less than 3 was recorded as 0, score greater than or equal to 3 was recorded as 1) to denoise the results. The sum of the thresholded score of each item was used as HEIGD.

## Modeling analysis of delay discounting task

For each delay, the choices were defined as 0 for choosing the immediate option and 1 for choosing the future option. Then logistic regression was used to determine the monetary amount at which there was a 0.5 probability of choosing the immediate versus the delayed option for the delay, which was the indifference point (1, 2).

The logistic function was defined as:

$$P(\text{delay}) = \frac{1}{1+e^{-\beta \times M}}$$

P(delay) is the probability of choosing the delayed option, β is a regression parameter to be estimated, M is the reward for delayed option, and e is Euler number.

The indifference point was used to derive the discounted value (DV):

$$DV = \frac{\text{magnitude of immediate reward}}{\text{indifference point}}$$

The magnitude of immediate reward in the present study was 50 Chinese yuan.

For the estimation of discounting rate, DVs were fit against the delays with a hyperbolic function:

$$DV = \frac{1}{1+D \cdot T}$$

T is the delays, and D is the discounting rate to be estimated.

## Modeling analysis of Iowa gambling task

**PVL-Decay model.**

The outcome evaluation follows the Prospect utility function:

$$u(t) = \begin{cases} x(t)^{\alpha} & \text{if } x(t) \geq 0 \\ -\lambda \left| x(t) \right|^{\alpha} & \text{if } x(t) < 0 \end{cases}$$

Here, u(t) is the utility of net outcome x(t) on trial t. α governs the shape of the utility function, and λ is loss aversion parameter which determines the sensitivity to losses compared to gains. Raw pay-offs within data are divided by 100 (default scale) (3).

Then the expectancy of the chosen deck is updated by the utility:

$$E_j(t+1) = A \cdot E_j(t) + \delta_j(t) \cdot u(t)$$

Here, $E_j(t)$ is the expectancy of deck j on trial t. A determines how much the past expectancy is discounted. $\delta_j(t)$ is a dummy variable which is 1 if deck j is chosen on trial t and 0 otherwise.
The softmax choice rule was used to estimate the probability of choosing deck j on trial t+1:

$$\Pr[\text{Choice}(t+1) = j] = \frac{e^{\theta \cdot E_j(t+1)}}{\sum_{n=1}^{4} e^{\theta \cdot E_n(t+1)}}$$

$\theta$ was set to $3^{cons}$-1. Here, 'cons' is a consistency parameter. Higher 'cons' indicates choices will depend more on current expectancy.

**PVL-Delta model.**

The PVL-Delta is the same as PVL-Decay except that it use a different updating rule:

$$E_j(t+1) = E_j(t) + k \cdot \delta_j(t) \cdot [u(t) - E_j(t)]$$

k determines the learning rate of prediction error.

**VPP model.**

The VPP model tracks both expectancies $E_j(t)$ and perseverance strengths $P_j(t)$. $E_j(t)$ is updated by the updating rule in PVL-Delta. For the updates of $P_j(t)$:

$$P_j(t+1) = \begin{cases} A \cdot P_j(t) + \varepsilon_p & \text{if } x(t) \geq 0 \\ A \cdot P_j(t) + \varepsilon_n & \text{if } x(t) < 0 \end{cases}$$

Here, A determines how much the past perseverance strength is discounted. $\varepsilon_p$ and $\varepsilon_n$ indicate the impact of gain and loss on perseverance behavior, respectively.
The overall value of deck j on trial t+1 is the weighted sum of expectancy and perseverance strength:

$$V_j(t+1) = w \cdot E_j(t+1) + (1-w) \cdot P_j(t+1)$$

The soft max rule was also used to estimate the probability of choosing deck j on trial t+1:

$$\Pr[\text{Choice}(t+1) = j] = \frac{e^{\theta \cdot V_j(t+1)}}{\sum_{n=1}^{4} e^{\theta \cdot V_n(t+1)}}$$

**ORL model.**

The ORL model tracks both expected value $EV_j(t)$ and expected win frequency $EF_j(t)$. $EV_j(t)$ is updated with separate learning rates for reward and punishment net outcomes:

$$EV_j(t+1) = \begin{cases} EV_j(t) + k_{rew} \cdot \delta_j(t) \cdot [x(t) - EV_j(t)] & \text{if } x(t) \geq 0 \\ EV_j(t) + k_{pun} \cdot \delta_j(t) \cdot [x(t) - EV_j(t)] & \text{if } x(t) < 0 \end{cases}$$

$k_{rew}$ and $k_{pun}$ are learning rates for reward and punishment outcomes, respectively.
$EF_j(t)$ is also updated with separate learning rates for reward and punishment outcomes:

$$EF_j(t+1) = \begin{cases} EF_j(t) + k_{rew} \cdot [\text{sgn}(x(t)) - EF_j(t)] & \text{if } x(t) \geq 0 \\ EF_j(t) + k_{pun} \cdot [\text{sgn}(x(t)) - EF_j(t)] & \text{if } x(t) < 0 \end{cases}$$

$k_{rew}$ and $k_{pun}$ are learning rates shared with the expected value learning rule, and sgn(x(t)) is a function which returns 1, 0, or −1 for positive, 0, or negative outcome values on trial t, respectively. For the unchosen decks j′ on trial t:

$$EF_{j'}(t+1) = \begin{cases} EF_{j'}(t) + k_{pun} \cdot [\frac{-sgn(x(t))}{C} - EF_{j'}(t)] & \text{if } x(t) \geq 0 \\ EF_{j'}(t) + k_{rew} \cdot [\frac{-sgn(x(t))}{C} - EF_{j'}(t)] & \text{if } x(t) < 0 \end{cases}$$

C is the number of possible alternative choices, which is 3 in the current study.

The ORL model also employs a simple choice perseverance model to capture decision makers' tendencies to stay or switch decks, irrespective to the outcome:

$$PS_j(t+1) = \begin{cases} \frac{1}{1+K} & \text{if Choice}(t) = j \\ \frac{PS_j(t)}{1+K} & \text{otherwise} \end{cases}$$

K is determined by:

$$K = 3^{K'} - 1$$

The overall value of deck j on trial t+1 is the weighted sum of expected value, expected win frequency, and perseverance strength:

$$V_j(t+1) = EV_j(t+1) + \beta_F \cdot EF_j(t+1) + \beta_P \cdot PS_j(t+1)$$

The soft max rule was also used to estimate the probability of choosing deck j on trial t+1:

$$Pr[Choice(t+1) = j] = \frac{e^{V_j(t+1)}}{\sum_{n=1}^{4} e^{V_n(t+1)}}$$

An R package hBayesDM v1.1.1, which is a decision-making task modeling package base on Stan framework, was used for the parameters estimation and model comparison.

## Brain network construction

Regional parcellation was applied to the preprocessed images using Automated Anatomical Labeling (AAL) template (4), which divided each cerebral hemisphere into 45 anatomical cortical and subcortical regions, each defined as a regional node in later analyses. A set of 90 regional mean time series were estimated for each individual by averaging the time series over all the voxels in given region. Then, Pearson correlation coefficients between regional time series were estimated to generate a correlation matrix for each subject. The absolute correlation matrices were used to construct binary undirected graphs. We firstly calculated the minimum spanning tree (MST) that connected all 90 regional nodes with 89 edges for each subject (5-7). Then, additional edges were added to the MST in the descending order of the correlation coefficients, yielding a series of networks with connection density ranging from 5% to 50% in increments of 1% (7). The MST-based networks have the unique advantage of producing networks containing the same number of connected nodes, thereby permitting group-level comparisons (5, 7).

## Hubness estimations

In order to introduce these graph measures, we first define some basic concepts: A represents the binary adjacency matrix corresponding to the brain network. $a_{ij}$ is an element in matrix A, and $a_{ij}$ = 1 indicates that there is an edge between node i and node j , $a_{ij}$ = 0 means that there is no connection between node i and node j. N represents the set of all nodes in the network, and n is the number of nodes in the network.

**Closeness centrality** of a node is calculated as the reciprocal of the average shortest path lengths between that node and other nodes in the network. Therefore, the higher the closeness centrality of a node, the higher the efficiency of information exchange between the node and other nodes in the network. The formula for calculating close centrality is as follows:

$$c_i = \frac{n-1}{\sum_{j\in N, j\neq i} l_{ij}}$$

$c_i$ is the closeness centrality of node i, $l_{ij}$ is the shortest path length between node i and node j.

**Degree centrality** of a node measures the number of nodes that form an edge with the node, so it can reflect the importance of the node in the network. The formula for calculating degree centrality is as follows:

$$d_i = \sum_{j\in N} a_{ij}$$

$d_i$ is the degree centrality of node i.

**Betweenness centrality** of a node measures the ratio of the shortest paths through the node to all shortest paths in the network. Therefore, the higher the betweenness centrality of a node, the more information exchanges between different regions in the network pass through the node, and the node plays a bridge-like role in the network architecture. The formula for calculating betweenness centrality is as follows:

$$b_i = \frac{1}{(n-1)(n-2)} \sum_{h,j\in N, h\neq j, h\neq i, j\neq i} \frac{\rho_{hj}(i)}{\rho_{hj}}$$

$b_i$ is the betweenness centrality of node i. $\rho_{hj}$ is the number of shortest paths between node h and node j. $\rho_{hj}(i)$ is the number of shortest paths between node h and node j that pass through node i.

**Eigenvector centrality** assigns relative scores to all nodes in the network based on the concept that connections to high-scoring nodes contribute more to the score of the node in question than equal connections to low-scoring nodes. It can be calculated by estimate the eigenvector of adjacency matrix:

$$Ae = Ze,$$

e is the eigenvector of matrix A, Z is the eigenvalue. The eigenvector with the highest eigenvalue was used as the eigenvector centrality of nodes in the network.

**Nodal efficiency** is calculated as the average of the reciprocal of the shortest path lengths between that node and other nodes in the network. It measures the average efficiency of information

exchange between the node and other nodes in the network. The calculation formula of node efficiency is as follows:

$$E_i = \frac{1}{n-1} \sum_{j \in N, j \neq i} \frac{1}{l_{ij}}$$

$E_i$ is the nodal efficiency of node i. $l_{ij}$ is the shortest path length between node i and node j.

## The Chinese version of the problem internet game playing questionnaire

请根据您的实际情况，用·0~5 分对过度网络游戏行为的程度进行评分。需要注意的是：每项两个分数，分别对应最近一周、以及一年内该行为最强烈时的情况。

| | | 最近一周 | 该行为在一年内最强烈时 |
|---|---|---|---|
| 1 | 我感到自己的身心被这种行为占据了 | | |
| | 当我不进行这种行为的时候，我还在回忆这种行为 | | |
| | 当我不进行这种行为的时候我还在考虑下一次怎么进行这种行为 | | |
| 2 | 我用来进行这种行为的时间越来越长 | | |
| 3 | 我曾试图控制自己，不进行这种行为或减少进行这种行为的时间，但没有成功 | | |
| | 我进行这种行为的时间超过自己的预计时间 | | |
| 4 | 如果在这种行为中没有获得自己想要的目标，我会为了这些目标继续进行下去 | | |
| 5 | 当我不能进行这种行为的时候，我感到易怒或心绪不宁 | | |
| 6 | 当我觉得紧张时，我会进行这种行为来消减紧张 | | |
| | 当我觉得悲伤时，我会进行这种行为来消减悲伤 | | |
| | 当我觉得生气时，我会进行这种行为来消减愤怒 | | |
| | 当我遇到麻烦时，我会进行这种行为来派遣烦恼 | | |
| 7 | 我向别人隐瞒我的这种行为，如：父母、朋友、老师或老板 | | |
| 8 | 为了进行这种行为，我逃课或旷工 | | |
| | 为了进行这种行为，我偷东西 | | |
| | 为了进行这种行为，我与别人争吵 | | |
| | 为了进行这种行为，我和别人打架 | | |
| 9 | 为了进行这种行为，我不能专心学习或工作 | | |
| | 为了进行这种行为，我不能按时按量吃饭 | | |
| | 为了进行这种行为，我不能按时按量睡觉 | | |
| | 为了进行这种行为，我与朋友在一起的时间变少了 | | |
| | 为了进行这种行为，我与亲人们在一起的时间变少了 | | |

For each section of the questionnaire, the highest score for the question within that section was used as the score for that section.

## References

1. Li N, Ma N, Liu Y, He XS, Sun DL, Fu XM, Zhang XC, Han SH, Zhang DR. Resting-state functional connectivity predicts impulsivity in economic decision-making. J Neurosci. 2013;33:4886-4895.
2. Zha RJ, Bu JJ, Wei ZD, Han L, Zhang PY, Ren JC, Li JA, Wang Y, Yang LZ, Vollstadt-Klein S, Zhang XC. Transforming brain signals related to value evaluation and self-control into behavioral choices. Hum Brain Mapp. 2019;40:1049-1061.
3. Li JA, Dong D, Wei Z, Liu Y, Pan Y, Nori F, Zhang X. Quantum reinforcement learning during human decision-making. Nat Hum Behav. 2020;4:294-307.
4. Tzourio-Mazoyer N, Landeau B, Papathanassiou D, Crivello F, Etard O, Delcroix N, Mazoyer B, Joliot M. Automated anatomical labeling of activations in SPM using a macroscopic anatomical parcellation of the MNI MRI single-subject brain. Neuroimage. 2002;15:273-289.
5. Alexander-Bloch AF, Gogtay N, Meunier D, Birn R, Clasen L, Lalonde F, Lenroot R, Giedd J, Bullmore ET. Disrupted modularity and local connectivity of brain functional networks in childhood-onset schizophrenia. Frontiers in Systems Neuroscience. 2010;4:147.
6. Chun-Yi Zac Loa T-WS, Chu-Chung Huanga, Chia-Chun Hungc,d, Wei-Ling Chenc, Tsuo-Hung Lanc, Ching-Po Lina,e,1, and Edward T. Bullmoref,g,h,i. Randomization and resilience of brain functional networks as systems-level endophenotypes of schizophrenia. P Natl Acad Sci USA. 2015;112:9123-9128.
7. He XS, Doucet GE, Pustina D, Sperling MR, Sharan AD, Tracy JI. Presurgical thalamic "hubness" predicts surgical outcome in temporal lobe epilepsy. Neurology. 2017;88:2285-2293.